Journal of Saudi Chemical Society (2014) **18**, 276–287

King Saud University

Journal of Saudi Chemical Society

www.ksu.edu.sa
www.sciencedirect.com

ORIGINAL ARTICLE

Optimization of the chemoenzymatic mono-epoxidation of linoleic acid using D-optimal design

Bashar Mudhaffar Abdullah, Nadia Salih, Jumat Salimon *

School of Chemical Sciences and Food Technology, Faculty of Science and Technology, Universiti Kebangsaan Malaysia, 43600 Bangi, Selangor, Malaysia

Received 7 February 2011; accepted 17 July 2011
Available online 22 July 2011

KEYWORDS

Linoleic acid;
Mono-epoxidation;
Novozym 435®;
D-optimal design

Abstract Mono-epoxied linoleic acid 9(12)-10(13)-monoepoxy 12(9)-octadecanoic acid (MEOA) was synthesized and optimized by immobilized *Candida antarctica* lipase (Novozym 435®) using D-optimal design. For optimizing the reaction, response surface methodology (RSM) was employed with four reaction variables such as the effect of amount of hydrogen peroxide (μL), amount of enzyme (w) and reaction time (h). At optimum conditions the experiment to obtain a higher yield% with a medium OOC% of MEOA was predicted at an amount of H_2O_2 μL of 15, Novozym 435® of 0.12 g and 7 h of reaction time. At this condition, the yield of MEOA was 82.14%, 4.91% of OOC and 66.65 mg/g of iodine value (IV). The observed value was reasonably close to the predicted value. Hydrogen peroxide was found to have the most significant effect on the degree of epoxidation OOC% and yield%. The epoxy ring opening (–C–O–C–) has been observed by Fourier Transform Infrared Spectroscopy (FTIR) at 820 cm^{-1} and the double band (–C═C–) at 3009 cm^{-1}. ^1H NMR analyses confirmed that the oxirane ring (–C*H*–O–C*H*–) of MEOA at 2.92–3.12 ppm and four signals of methane (–C*H*═C*H*–) was at 5.38–5.49 ppm while the ^{13}C NMR showed the oxirane ring (–C–O–C–) at 54.59–57.29 ppm and the olefinic carbons at 124.02–132.89 ppm.

* Corresponding author. Tel.: +60 3 8921 5412; fax: +60 3 8921 5410.
E-mail address: jumat@ukm.my (J. Salimon).

Peer review under responsibility of King Saud University.
doi:10.1016/j.jscs.2011.07.012

Production and hosting by Elsevier

1. Introduction

Epoxidation of vegetable oils compose a useful alternative to petroleum based epoxides, because of their lower toxicity and availability from renewable resources. Epoxidized vegetable oils are used for several applications such as plasticizers, polyurethane production (Joseph et al. 2004, John et al. 2002 and Benaniba et al. 2003), reactive diluents for paints, as protection agents (Ahmad et al. 2002), surfactants (Warwel & Bruese, 2004), and as additives to biolubricant baseoils (Adhvaryu & Erhan, 2002).

Epoxidized vegetable oils are produced by epoxidation of unsaturated vegetable oils; such as soybean, linseed oil (Ruesch et al. 1999) and *Jatropha curcas* seed oil (Meyer et al. 2008). In spite of there are several methods available to epoxidize the unsaturated fatty acids such as oleic and linoleic acids, the only method used on industry is the (Prileshajev) epoxidation reaction. In this reaction a peracid from a short chain fatty acid and hydrogen peroxide (H_2O_2) under strong acidic conditions is used as the oxidizing agent. In spite of a carful choice of the epoxidation reaction conditions can help to minimize the epoxides loss and the selectivity of industrial epoxidation of vegetable oils scarcely exceeds 80% (Ruesch et al. 1999).

In the lipase catalyze for epoxidation of unsaturation fatty acid, the acid itself reacts with H_2O_2 to form the peracid, which then epoxidized the double bond. The reaction is therefore often referred to as 'self-epoxidation reaction', in spite of the fact that the second step proceeds predominantly via an intermolecular process (Klass & Warwel 1997 and Warwel & Klass 1995). Among the several lipases studied, *Candida Antarctica* lipase B (Novozym 435®) has been shown to be the most effective (Orellana-Coca et al. 2005).

This chapter focuses on the impact of various reaction parameters on the mono-epoxidation process, with the aim to determine the optimal reaction conditions with regard to reaction efficiency and enzyme stability using D-optimal design. Linoleic acid (LA; 18:2) was used as the model substrate. Figure 1 demonstrates the scheme for the mono-epoxidation reaction of LA. Mono-epoxidation of LA results in the mixture of two mono-epoxides (cis-9, 10-epoxy 12c- 18:1 and cis-12, 13 epoxy 9c- 18:1).

2. Methodology

2.1. Experimental procedure

The enzymatic mono-epoxidation was carried out using Novozym 435®, a commercial catalyst made up of lipase, from *C. antarctica*, immobilized on a polyacrylate resin (Orellana-Coca et al., 2005). Table 1 shows the different ratio of hydrogen peroxide, different weight of enzyme and different time using D-optimal design. 3-Factors (variables), such as hydrogen peroxide (μL, X_1), enzyme (g, X_2) and time (h, X_3) were performed under the same experimental conditions. In a typical chemo-enzymatic mono-epoxidation of linoleic acid 9(12)-10(13)-monoepoxy 12(9)-octadecanoic acid (MEOA), the linoleic acid (1.4 g) was dissolved in 10 mL toluene and the lipase was added. After stirring for 15 min 30% H_2O_2 were added, and every 15 min the addition was repeated. Afterward the lipase was removed by filtration, the mixture was washed with water to remove excess H_2O_2 and the organic phase was dried over anhydrous sodium sulfate, and solvent was evaporated in a vacuum rotary evaporator. The yield%, oxirane ring content% and iodine value was measured, on the other hand the FTIR and ^1H, ^{13}C NMR were analyzed.

2.2. Experimental design and statistical analysis

To explore the effect of the operation variables on the response in the region of investigation, a D-optimal design at three levels was performed. Hydrogen peroxide (μL, X_1), amount of enzyme (g, X_2) and reaction time (h, X_3) were selected as

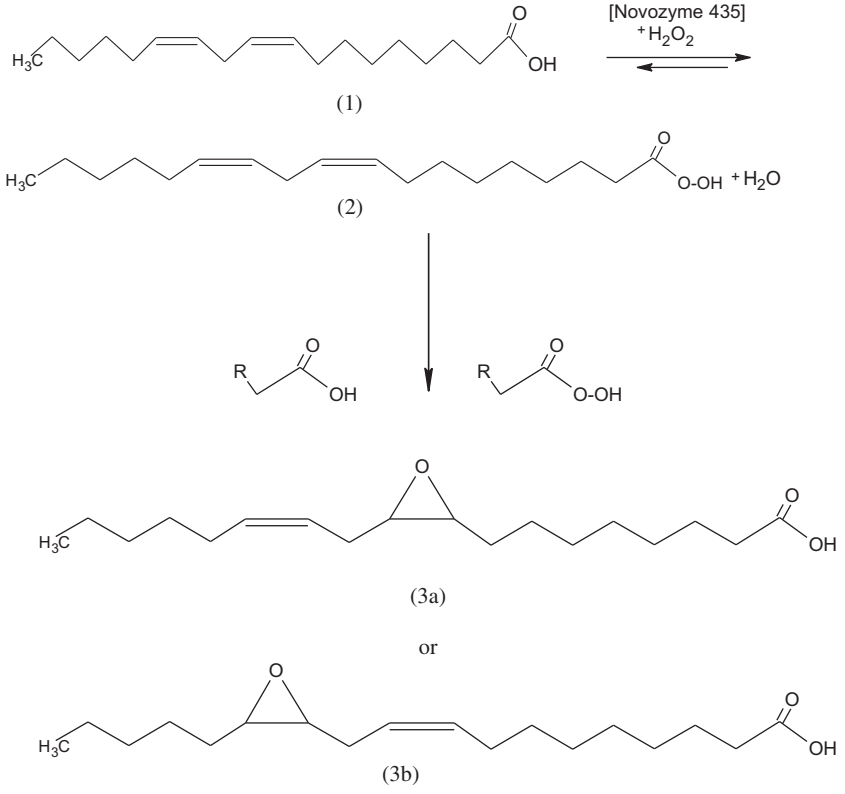

Figure 1 Chemo-enzymatic MEOA. Notes: linoleic acid (1); perlinoleic acid (2); 9-10-monoepoxy 12-octadecenoic acid (3a); 12-13-monoepoxy 9-octadecenoic acid (3b).

Table 1 Independent variables and their levels for D-optimal design of the mono-epoxidation reaction.

Independent variables		Variable Levels		
		−1	0	+1
H_2O_2 (μL)	X_1	15	17.5	20
Enzyme (g)	X_2	0.08	0.1	0.12
Time (h)	X_3	6	7	8

independent variables. The range of values and coded levels of the variables are given in Table 1.

A polynomial equation was used to predict the response as a function of independent variables and their interactions. In this work, the number of independent variables was three and, therefore, the response for the quadratic polynomials becomes:

$$Y = \beta_0 + \sum \beta_i x_i + \sum \beta_{ii} x_i^2 + \sum \sum \beta_{ij} x_i x_j \quad (1)$$

where β_0; β_i; β_{ii} and β_{ij} are constant, linear, square and interaction regression coefficient terms, respectively, and xi and xj are independent variables. The Minitab software version 14 (Minitab Inc., USA) was used for multiple regression analysis, analysis of variance (ANOVA), and analysis of ridge maximum of data in the response surface regression (RSREG) procedure. The goodness of fit of the model was evaluated by the coefficient of determination R^2 and its statistical significance that was checked by the *F*-test.

3. Results and discussion

This study demonstrates the application of the proposed RSM framework for the optimization of linoleic acid by using Novozym 435® catalytic oxidation process. Hence, the knowledge about the process is relatively limited, and the design is used to obtain 18 design points within the whole range of three factors for experiments. The designs and the responses yield% of MEOA (Y_1), OOC% (Y_2) and IV mg/g (Y_3) are given in Table 2.

Following the reaction experiments, the response surface is approximated by D-optimal design. Hydrogen peroxide is an important reactant for the formation of peracids from fatty acids; hence, the influence of its amount on the mono-epoxidation reaction was studied. The addition of H_2O_2 solution to the reaction medium (toluene with linoleic acid) leads to the formation of two distinct phases: an organic phase and an aqueous phase.

The Novozym 435®, being adsorbed on a hydrophobic carrier, is mainly present in the organic phase, while H_2O_2 will be partitioned in both the aqueous and the organic phases, with the concentration being higher in the aqueous phase (Fig. 2) due to consumption of H_2O_2 for the peracid formation in the organic phase, the ratio of H_2O_2 to H_2O tends to decrease slightly in the organic phase. Hence, for the reaction to proceed optimally, it is essential that the transport of the peroxide from the aqueous phase to the organic phase is faster than its utilization in the enzymatic reaction (Orellana-Coca et al., 2005). This was determined performing varying amounts of H_2O_2 (15, 17.5 and 20 μL) which have been added every 15 min, the addition was repeated 24 times, Novozym 435® (0.08, 0.10 and 0.12 g) and different time (6, 7 and 8 h). A stoichiometric excess of the required amount of the peroxide was used to compensate for its possible decomposition by light and temperature.

Table 2 shows that the yield percentage of MEOA, Y_1 has increased to 82.14% while OOC%, Y_2 4.91 and iodine value, Y_3 66.65 which considerably compared to the theoretical (OOCt) 9.02% and the initial iodine value (IV_0) 157.35 mg/g. Subsequent experiments were performed using different

Table 2 D-optimal design arrangement and responses for MEOA.

Run no.	H_2O_2 (X_1)	Catalyst[a] (X_2)	Time[b] (X_3)	*YI*, yield (%)	Y_2, OOC (%)	RCO (%)	Y_3, IV (mg/g)	X (%)	SE
1	20.00	0.08	8	76.57	6.17	68.4	37.81	76.37	0.89
2	17.5	0.08	7	88.57	5.48	60.75	58.95	62.53	0.97
3	17.5	0.10	8	72.14	7.54	83.59	32.22	79.52	1.05
4	20.00	0.08	6	72.28	6.4	70.95	40.98	73.95	0.95
5	20.00	0.12	7	54.71	5.94	65.85	64.32	59.12	1.11
6	20.00	0.12	6	60.28	7.88	87.36	30.87	80.38	1.08
7	15.00	0.12	8	73.57	5.48	60.75	53.24	66.16	0.91
8	20.00	0.08	7	81.42	5.37	59.53	56.32	64.2	0.92
9	15.00	0.10	7	75.68	5.02	55.65	74.64	52.56	1.05
10	18.75	0.10	7	85.28	5.71	63.3	49.17	68.75	0.92
11	20.00	0.10	7	81.14	6.05	67.06	42.72	72.85	0.92
12	15.00	0.12	6	70.78	4.57	50.66	76.48	51.39	0.98
13	15.00	0.10	6	65.93	3.65	40.46	96.43	38.71	1
14	15.00	0.12	7	82.14	4.91	54.43	66.65	57.64	0.94
15	17.5	0.12	8	59.28	6.74	74.72	36.37	76.63	0.97
16	20.00	0.10	6	72.85	6.51	72.17	39.76	74.73	0.9
17	15.00	0.08	8	77.14	4.34	48.11	83.85	46.71	1.03
18	17.5	0.10	6	80.85	3.77	41.79	87.09	44.65	0.93

Notes: OOC, oxirane oxygen content; RCO, relative percentage conversion to oxirane; IV, iodine value; X, conversion to double bond; SE, oxirane oxygen selectivity.

[a] Catalyst Novozym 435® (g).

[b] Epoxidation time (h).

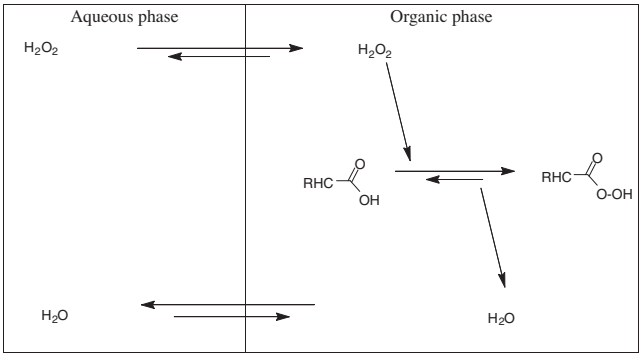

Figure 2 Schemitic presentation of the mass transport of hydrogen peroxide and water in an organic-water biphasic system.

amounts of H_2O_2 15, 17.5 and 20 μL for every 1.4 g of linoleic acid in one single step.

As seen in the Table 2, there was a clear increase in the reaction rate (OOC%) and decrease (IV mg/g) with increasing H_2O_2 amount. With 15 μL, mono-epoxidation was achieved at 7 h with using 0.12 g Novozym 435®, while total epoxidation was observed within 10 h using 30 μL. Increasing the peroxide amount used for the reaction results in increases of the peracid formation. In the state of partial epoxidation, the amount of peracids accumulated is not significant (less than 2% of the total) (Warwel and Klaas, 1995), because the chemical reaction in which they are consumed is very fast. But once all the double bonds are epoxidized, the remaining peracid is not consumed. As seen in Table 2, the effect of catalysts amount (Novozym 435®) was studied, which could indicate that at high catalyst amount, the utilization of H_2O_2 is so fast that the epoxidation of the double bonds does not keep pace with peracid formation.

The quadratic regression coefficients obtained by employing a least squares method technique to predict quadratic polynomial models for the yield% of MEOA (Y_1), OOC% (Y_2) and IV mg/g (Y_3) are given in Tables 3–5. For the yield% of MEOA (Y_1), the linear term of Novozym 435® catalyst amount (X_2), quadratic terms of H_2O_2 (X_{11}) and Novozym 435® catalyst amount (X_{22}) were significant ($p < 0.05$). The interaction between H_2O_2 (X_{11}) and Novozym 435® catalyst amount (X_{12}), and the interaction between H_2O_2 (X_{11}) and reaction time (X_{13}) were significant ($p < 0.05$), while its quadratic term of reaction time (X_{33}) was highly significant ($p < 0.01$).

Highly significant ($p < 0.01$) terms of OOC% (Y_2) and IV mg/g (Y_3) for the H_2O_2 (X_1) were linear, while linear term of IV mg/g for the reaction time h (X_3) was significant

Table 4 Regression coefficients of the predicted quadratic polynomial model for response variables of the OOC% for the MEOA.

Variables	Coefficients (β), OOC% (Y_2)	T	P	Notability
Intercept	5.59	2	0.1717	
Linear				
X_1	1	12.15	0.0082	***
X_2	0.58	3.25	0.1091	
X_3	0.51	2.54	0.1494	
Quadratic				
X_{11}	−0.37	0.36	0.5626	
X_{22}	−0.099	0.036	0.8546	
X_{33}	0.31	0.41	0.5404	
Interaction				
X_{12}	−0.22	0.26	0.6267	
X_{13}	−0.55	1.50	0.2553	
X_{23}	−0.27	0.31	0.5934	
R^2	0.69			

Notes: X_1 = amount of H_2O_2; X_2 = catalyst Novozym 435®; X_3 = reaction time; $^{**}P < 0.05$; T: F test value. See Table 2 for a description of the abbreviations.
*** $P < 0.01$.

Table 3 Regression coefficients of the predicted quadratic polynomial model for response variables of the yield% of MEOA.

Variables	Coefficients (β), yield% of MEOA (Y_1)	T	P	Notability
Intercept	87.53	8.22	0.0034	***
Linear				
X_1	−2.82	4.91	0.0575	
X_2	−4.5	10.07	0.0131	**
X_3	−0.14	0.01	0.9219	
Quadratic				
X_{11}	−9.06	10.82	0.011	**
X_{22}	−5.43	5.41	0.0485	**
X_{33}	−9.81	21.03	0.0018	***
Interaction				
X_{12}	−9.74	25.22	0.001	***
X_{13}	−7.14	12.99	0.0069	***
X_{23}	−7.8	12.83	0.0072	***
R^2	0.9			

Notes: X_1 = amount of H_2O_2; X_2 = catalyst Novozym 435®; X_3 = reaction time; See Table 2 for a description of the abbreviations. T: F test value.
** $P < 0.05$.
*** $P < 0.01$.

Table 5 Regression coefficients of the predicted quadratic polynomial model for response variables of the IV mg/g for the MEOA.

Variables	Coefficients (β), IV mg/g (Y_3)	T	P	Notability
Intercept	56.24	3.42	0.0489	**
Linear				
X_1	−18.82	21.45	0.0017	***
X_2	−8.91	3.87	0.0849	
X_3	−10.57	5.47	0.0474	**
Quadratic				
X_{11}	8.06	0.84	0.3865	
X_{22}	4.15	0.31	0.5935	
X_{33}	−4.41	0.42	0.5369	
Interaction				
X_{12}	11.59	3.5	0.0985	
X_{13}	10.81	2.92	0.1259	
X_{23}	5.42	0.61	0.458	
R^2	0.79			

Notes: X_1 = amount of H_2O_2; X_2 = catalyst Novozym 435®; X_3 = reaction time; T: F test value. See Table 2 for a description of the abbreviations.
** $P < 0.05$.
*** $P < 0.01$.

Table 6 Analysis of variance, showing the effect of the variables as linear, square and interactions on the response Y_1 (yield% of MEOA) of the D-optimal design.

Source	*Df*	Sum of squares	Mean square	*F* value	*P*
Mean	1	98362.39	98362.39		
Linear	3	530.07	176.69	2.72	0.0839
2FI	3	144.05	48.02	0.69	0.5763
Quadratic	3	623.88	207.96	11.85	0.0026
Lack-of-fit	8	140.36	17.55		
Pure error	18	99800.75	5544.49		

Table 7 Analysis of variance, showing the effect of the variables as linear, square and interactions on the response Y_2 (OOC% of MEOA) of the D-optimal design.

Source	*Df*	Sum of squares	Mean square	*F* value	*P*
Mean	1	572.69	572.69		
Linear	3	13.62	4.54	6.74	0.0048
2FI	3	1.43	0.48	0.66	0.5956
Quadratic	3	0.89	0.30	0.34	0.8001
Lack-of-fit	8	7.1	0.89		
Pure error	18	595.73	33.10		

Table 8 Analysis of variance, showing the effect of the variables as linear, square and interactions on the response Y_3 (IV mg/g of MEOA) of the D-optimal design.

Source	*Df*	Sum of squares	Mean square	*F* value	*P*
Mean	1	58695.37	58695.37		
Linear	3	4423.70	1474.57	8.18	0.0022
2FI	3	734.74	244.91	1.51	0.2672
Quadratic	3	354.25	118.08	0.66	0.5999
Lack-of-fit	8	1433.69	179.21		
Pure error	18	65641.75	3646.76		

($p < 0.05$). The coefficients of independent variables (amount of H_2O_2; X_1, catalyst Novozym 435®; X_2, and reaction time; X_3) were determined for the quadratic polynomial models Tables 3–5.

The lack of fit F-value for all the responses showed that the lack of fit is not significant ($p > 0.05$) relative to the pure error. This indicates that all the models predicted for the responses were adequate. Regression models for data on responses Y_1, Y_2, and Y_3, were highly significant ($p < 0.01$) with satisfactory R^2. However, R^2 for Y_2 (0.69) was lower although the model was significant. Tables 6–8 summarizes the analysis of variance (ANOVA) of all the responses of this study.

These results suggest that linear effect of hydrogen peroxide is the primary determining factor for MEOA. Orellana-Coca et al., (2005) also concluded that this variable had a very large effect on the results of their mono-epoxidation study. Final equations in terms of actual factors are:

$$Y_1 = +87.53 - 2.82X_1 - 4.50X_2 - 0.14X_3 - 9.06X_1^2 - 5.43X_2^2 - 9.81X_3^2 - 9.74X_1X_2 - 7.14X_1X_3 - 7.80X_2X_3 \quad (2)$$

$$Y_2 = +5.59 + 1.00X_1 + 0.58X_2 + 0.51X_3 - 0.37X_1^2 - 0.099X_2^2 + 0.31X_3^2 - 0.22X_1X_2 - 0.55X_1X_3 - 0.27X_2X_3 \quad (3)$$

$$Y_3 = +56.24 - 18.82X_1 - 8.91X_2 - 10.57X_3 + 8.06X_1^2 + 4.15X_2^2 4.41X_3^2 + 11.59X_1X_2 + 10.81X_1X_3 + 5.42X_2X_3 \quad (4)$$

RSM is one of the best ways of evaluating the relationships between responses, variables and interactions that exist. Significant interaction variables in the fitted models (Tables 3–5) were chosen as the axes (amount of H_2O_2; X_1, catalyst Novozym 435®; X_2 and reaction time X_3) for the response surface plots. The relationships between independent and dependent variables are shown in the three-dimensional representation as response surfaces. In a contour plot, curves of equal response values are drawn on a plane whose coordinates represent the levels of the independent factors. Each contour represents a specific value for the height of the surface above the plane defined for a combination of the levels of the factors. Therefore, different surface height values enable one to focus attention on the levels of the factors at which changes in the surface height occur (Wanasundara and Shahidi, 1999).

Canonical analysis was performed on the predicted quadratic polynomial models to examine the overall shape of the response surface curves and used to characterize the nature of the stationary points. Canonical analysis is a mathematical approach used to locate the stationary point of the response surface and to determine whether it represents a maximum, minimum or saddle point (Wanasundara and Shahidi, 1999; Mason et al., 1989).

Figs. 3–5 are the Design–Expert plots for all the responses. In the MEOA, performing the technique using low amount of H_2O_2 would give the desired OOC% of MEOA as shown in Fig. 4, while IV (Fig. 5) was higher at this condition. As shown in Figs. 4 and 5, the increasing amount of H_2O_2 led to increase of the OOC% and reduction of percentage of IV mg/g. The relationships between the parameters and MEOA were linear or almost linear. High OOC% could be obtained by using high

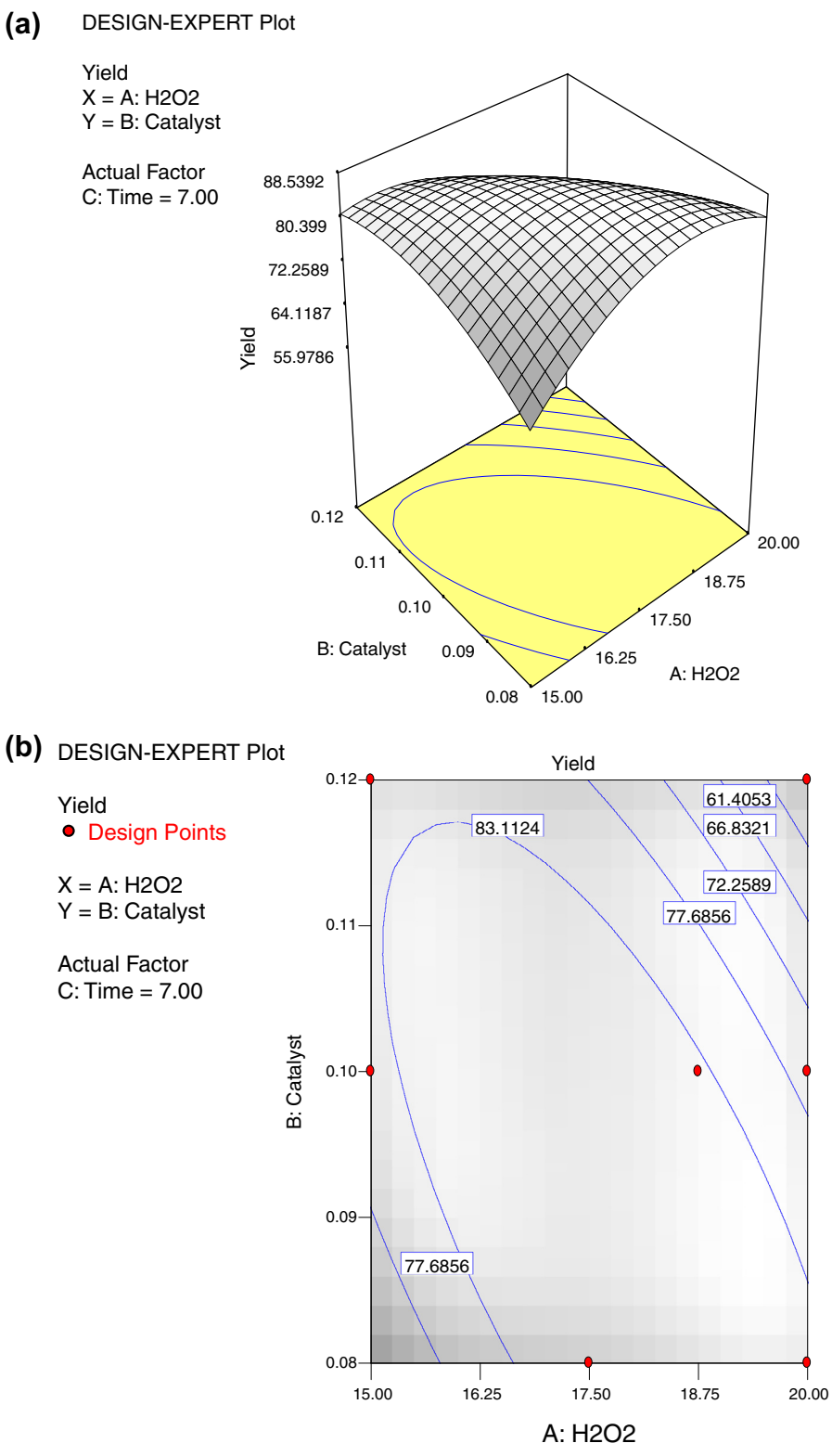

Figure 3 (a) Response surface and (b) contour plots for the effect of the H_2O_2 (X_1, μL) and catalysts Novozym 435® (X_2, g) on the yield% of MEOA.

amount of H_2O_2 at high reaction time. Experimental variables should be carefully controlled in order to recover a medium percentage of MEOA of interest with reasonable yield (Orellana-Coca et al., 2005).

Optimum conditions of the experiment to obtain higher yield% of MEOA and medium OOC% were predicted at amount of H_2O_2 μL of 15, catalyst Novozym 435® of 0.12 g and 7 h of reaction time. At this condition, the yield% of

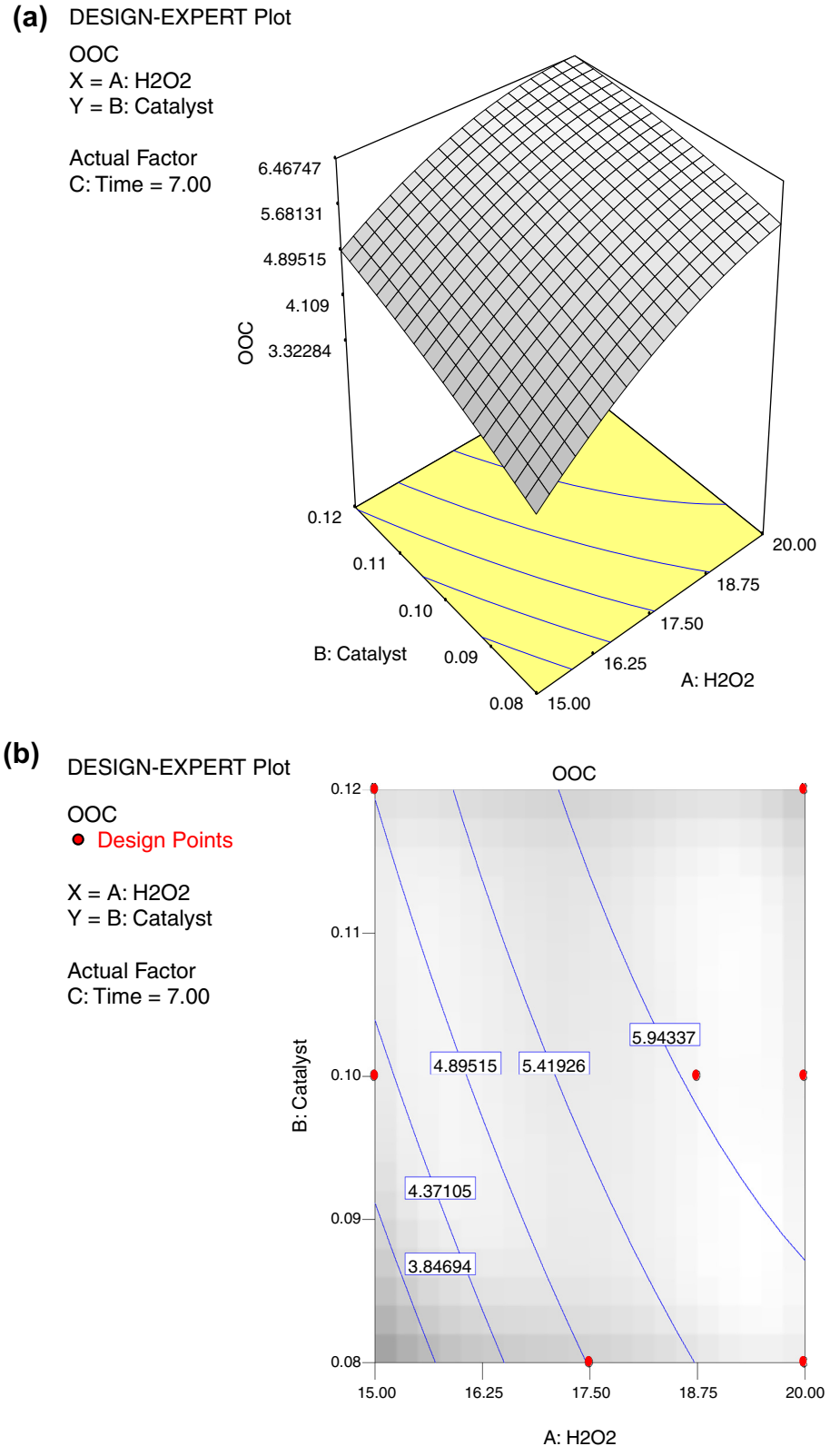

Figure 4 (a) Response surface and (b) contour plots for the effect of the H_2O_2 (X_1, μL) and catalysts Novozym 435® (X_2, g) on the OOC% of MEOA.

MEOA was 82.14%, 4.91% of OOC and 66.65 mg/g of IV. The observed value was reasonably close to the predicted value as shown in Figs. 6–8.

In order to prove the presence of oxirane ring of MEOA, final product was tested by FTIR. The comparison between linoleic acid (a) and MEOA (b), FTIR spectra is shown in

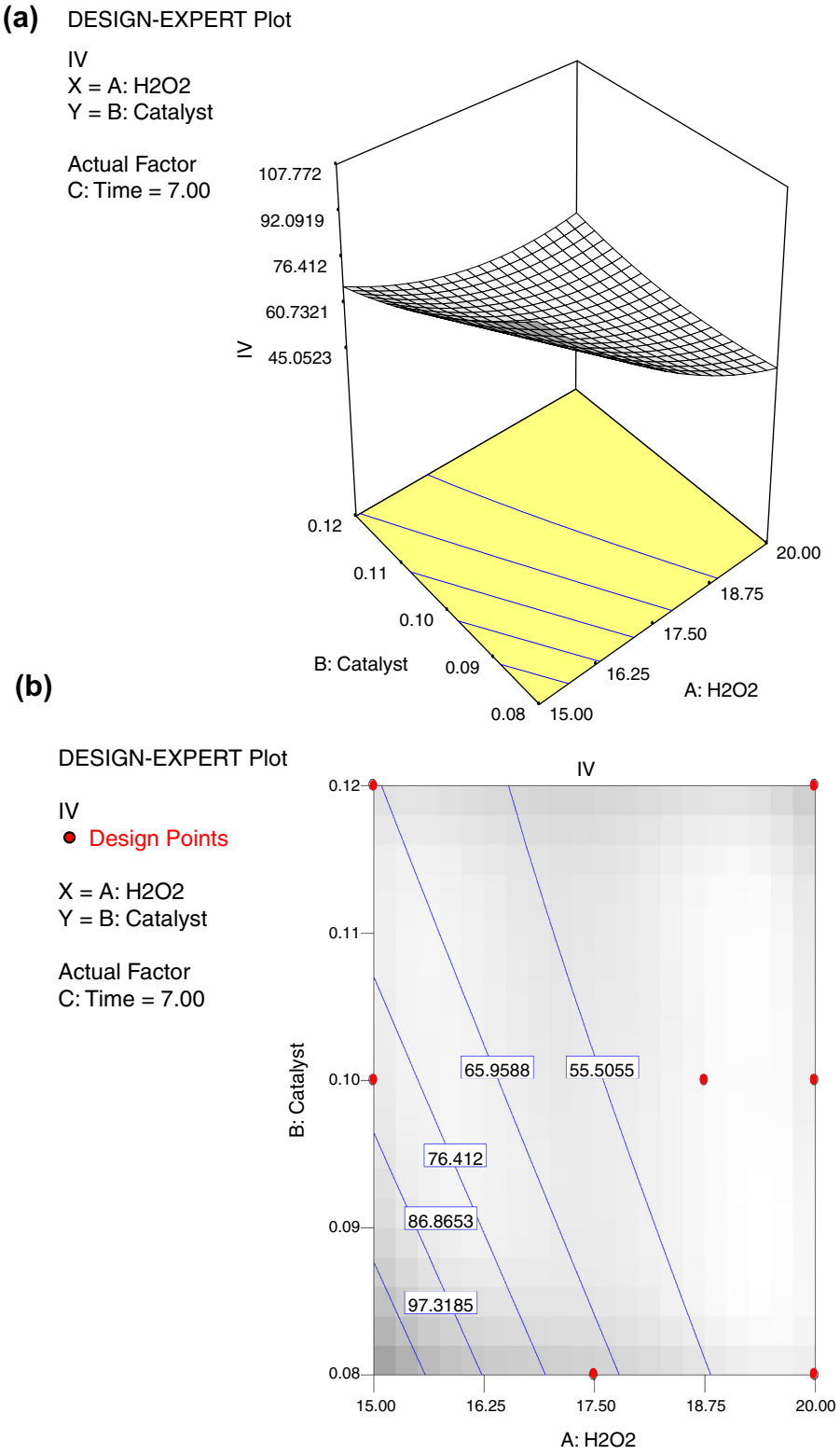

Figure 5 (a) Response surface and (b) contour plots for the effect of the H_2O_2 (X_1, μL) and catalysts Novozym 435® (X_2, g) on the IV mg/g of MEOA.

Fig. 9. The main peaks and their assignment to functional groups are given in Table 9. Oxirane ring of MEOA can be detected at wave number 820 cm^{-1}.

For the carboxylic acid carbonyl functional groups (C═O), FTIR spectrum showed absorption bands of linoleic acid and MEOA at 1719 and 1711 cm^{-1}, respectively, while stretching

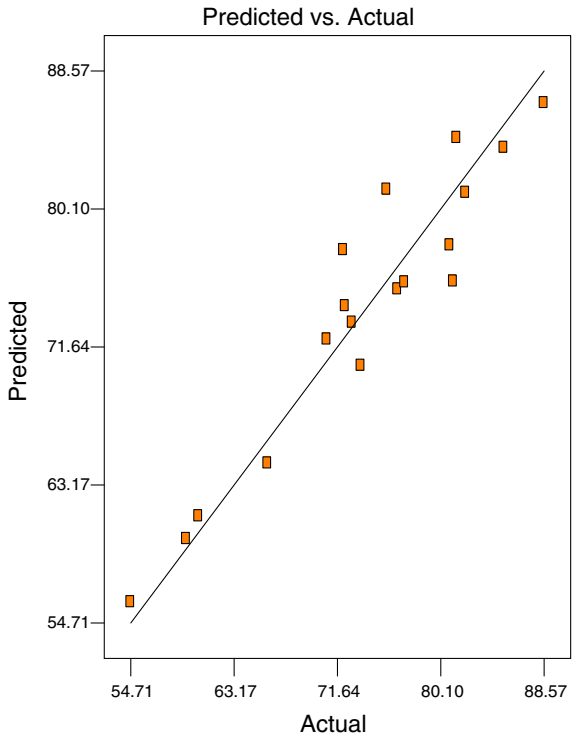

Figure 6 Prediceted vs. actual plot of Y_1.

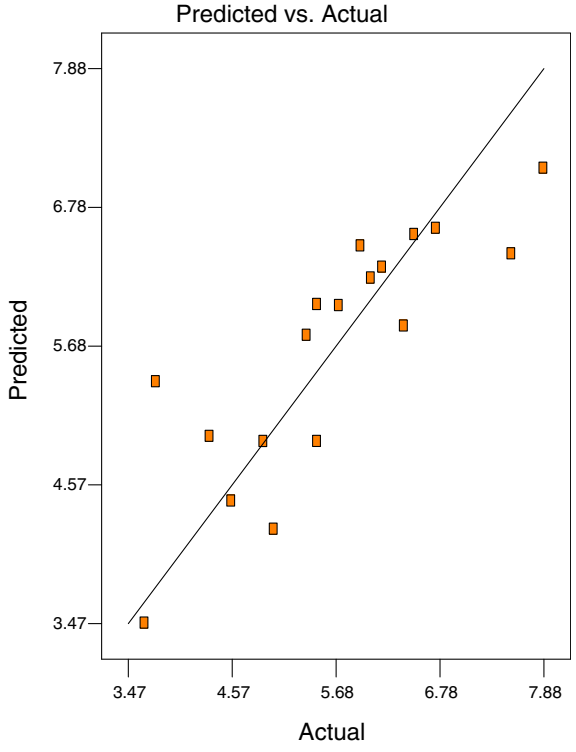

Figure 7 Prediceted vs. actual plot of Y_2.

vibration peak of C═C can be detected at wave number and 3009 cm^{-1}, respectively, (Socrates, 2001) and Peaks at 2927–2856 cm^{-1} indicated the CH_2 and CH_3 scissoring of linoleic acid and MEOA based on Fig. 9a and b. FTIR spectrum also

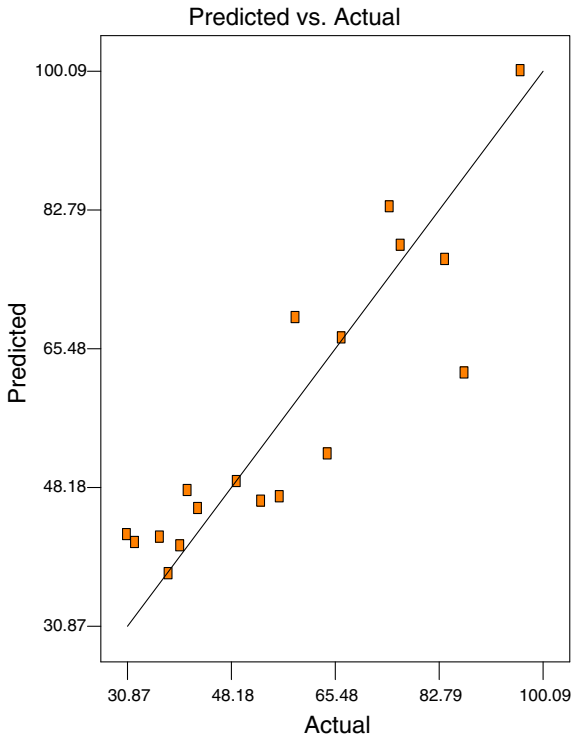

Figure 8 Prediceted vs. actual plot of Y_3.

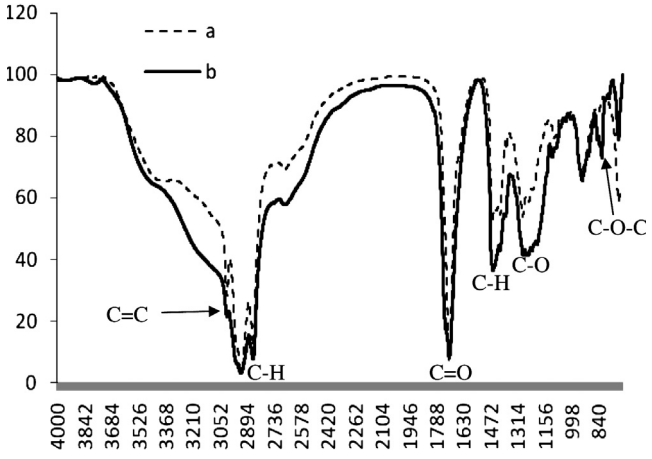

Figure 9 FTIR spectrum of the (a) linoleic acid and (b) MEOA.

Table 9 The main wavelengths in the FTIR functional groups of linoleic acid and MEOA.

Wavelength of LA	Wavelength of MEOA	Functional group
3009	3009	C═C bending vibration (aliphatic)
2927, 2855	2927, 2856	C–H stretching vibration (aliphatic)
1719	1711	C═O stretching vibration (carboxylic acid)
1454	1454	C–H scissoring and bending for methylene group
1284	1284	C–O stretching asymmetric (carboxylic acid)
937	934	C–H bending vibration (alkene)
—	820	C–O–C oxirane ring
722	723	C–H group vibration (aliphatic)

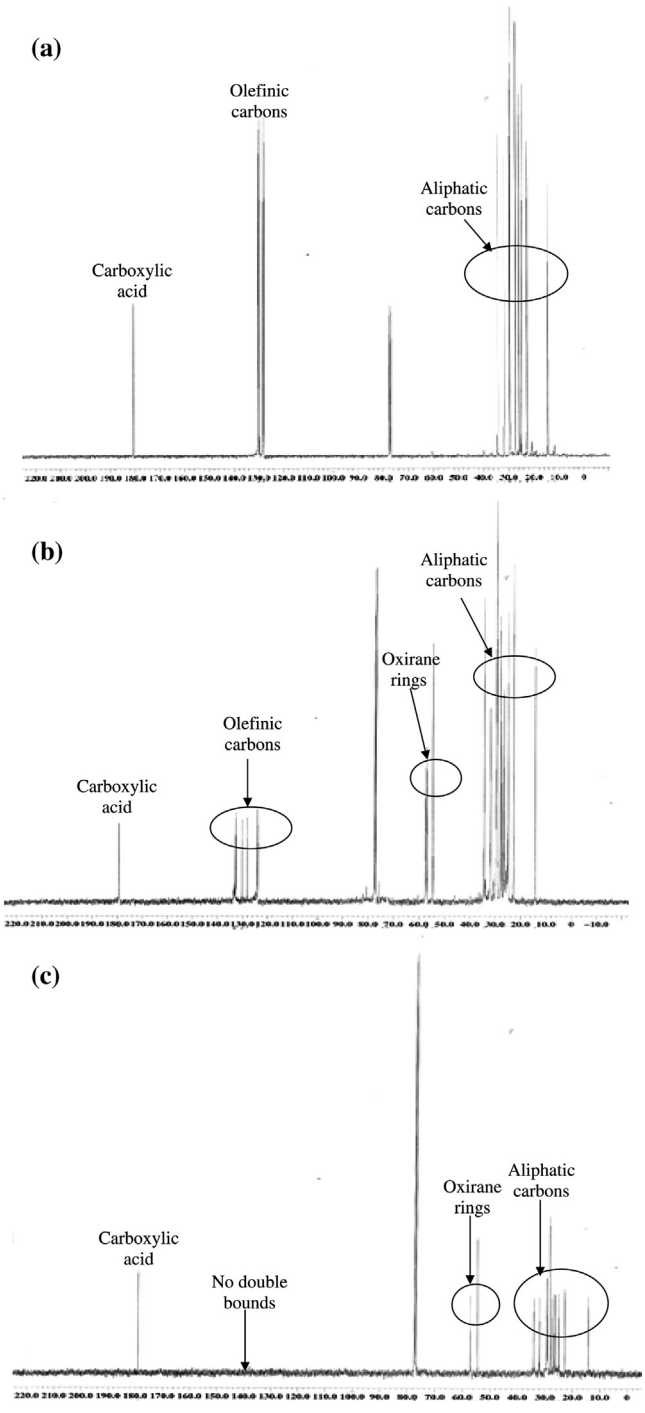

Figure 10 ^{13}C NMR spectrum of linoleic acid (a), MEOA (b) and di-epoxide linoleic acid (c).

showed absorption bands at 722, 723 for (C–H) group vibration.

3.1. ^{13}C NMR analysis

There has been recently a great interest in ^{13}C NMR spectroscopy of fatty acids as features in the spectra can be assigned to carbon atom. ^{13}C NMR spectroscopy being one of the less naturally-abundant isotopes of carbon also exhibits the phenomenon but until comparatively recent development in instrumentation and data processing have been made, ^{13}C NMR spectroscopy is now much more accessible and since all carbon atoms in the organic compounds give distinctive signals, whether or not they are linked to protons, a great deal of structural information can be obtained from the spectra.

Fig. 10a indicates the ^{13}C NMR spectrum of linoleic acid. The ^{13}C spectroscopy shows the main signals assignment of the linoleic acid as shown in Table 10. The signals at 180.49 ppm refer to the carbon atom of the carbonyl group (carboxylic acid). The signals at 128.27–130.38 ppm refer to the unsaturated carbon atoms (olefinic carbons); 24.86–29.79 ppm due to methylene carbon atoms in fatty acid moieties of linoleic acid (Abdullah and Salimon, 2009).

Fig. 10b and c can be confirmed the oxirane ring of MEOA 54.59–57.29 ppm and di-epoxide linoleic acid at about 54.61–57.32 ppm. Indeed, it appeared that the signals were present in the MEOA, as four peaks of roughly equal intensity (132.89, 132.72, 130.15, and 124.02 ppm) were observed in the alkenic carbon region in the ^{13}C-NMR spectrum Fig. 10b, while disappeared in the di-epoxide linoleic acid Fig. 10c (Du et al., 2004). The ^{13}C-NMR spectra indicate the existence of carbonyl group (carboxylic acid) in their structure mono-epoxide 179.32 ppm and di-epoxide at about 178.79 ppm. The other distinctive signals were aliphatic carbons MEOA at about 22.69–29.38 ppm and di-epoxide linoleic acid at about 22.77–29.44 ppm, which are common for these types of compounds (Doll et al., 2007).

3.2. ^{1}H NMR analysis

Proton magnetic resonance spectroscopy is the most valuable form of the technique for lipid analysis. The frequency at which any given hydrogen atom in an organic compound resonates is strongly dependent on its precise molecular environment. The ^{1}H NMR spectroscopy shows the main signals assignments in linoleic acid, MEOA and di-epoxide linoleic acid as shown in Table 11.

The ^{1}H NMR spectra for the products show some of the key features for a typical of (–C*H*–O–C*H*–) at about 2.92–3.12 ppm of MEOA and about 2.99–3.13 ppm of di-epoxide

Table 10 The main signals present in ^{13}C NMR functional groups of linoleic acid, MEOA and di-epoxide linoleic acid.

δ (ppm) Linoleic acid	δ (ppm) MEOA	δ (ppm) Di-epoxide linoleic acid	Assignment
24.86–29.79	22.69–34.15	22.77–29.44	–CH_2–carbons
—	54.59–57.29	54.61–57.32	() epoxide groups
128.27–130.38	124.02–132.89	—	–CH=CH–olefinic carbons
180.49	179.32	178.79	C=O carboxylic acid

Table 11 The main signals present in ^{1}H NMR functional groups of linoleic acid, MEOA and di-epoxide linoleic acid.

δ (ppm) Linoleic acid	δ (ppm) MEOA	δ (ppm) Di-epoxide linoleic acid	Assignment
0.88–0.91	0.86–0.88	0.88–0.92	–C*H*$_3$
1.30–2.77	1.29–2.33	1.34–2.36	–C*H*$_2$
–	2.92–3.12	2.99–3.13	–C*H*–O–C*H*–
5.35–5.36	5.38–5.49	—	–C*H*═C*H*–
7.27	7.27	7.27	–COO*H*

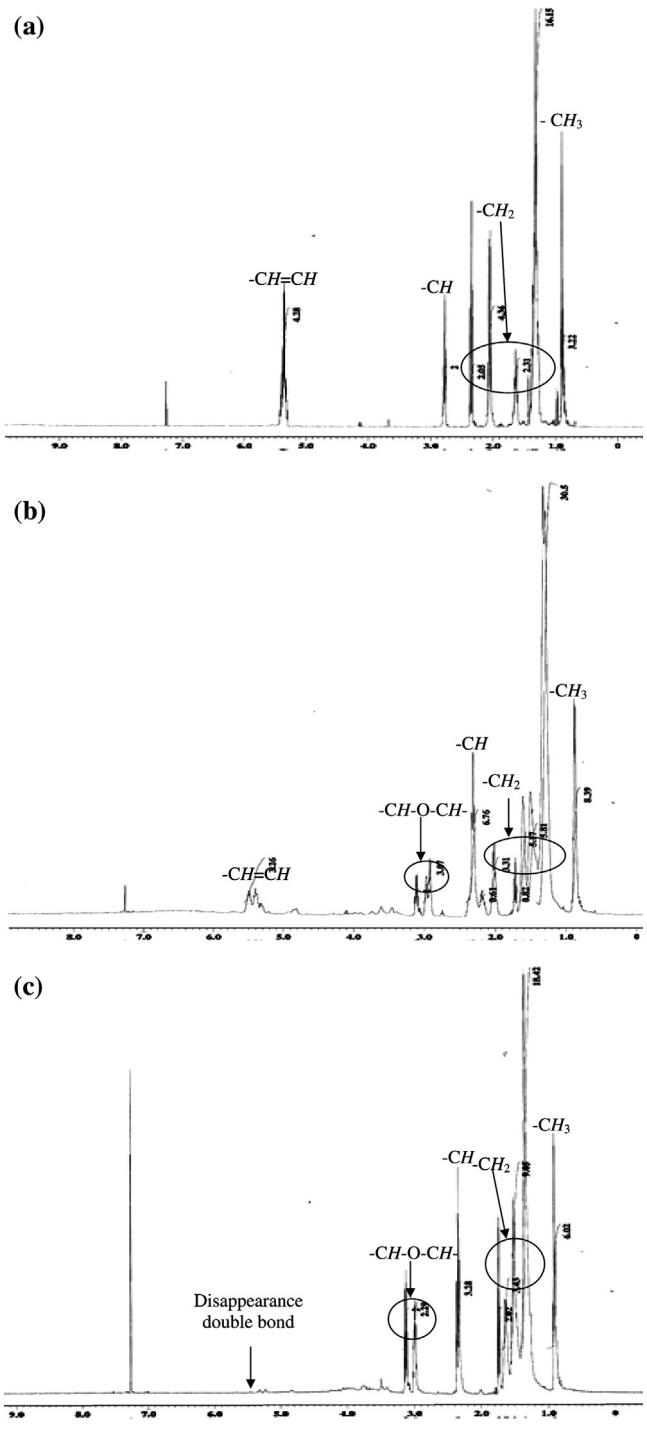

Figure 11 ^{1}H NMR spectrum of linoleic acid (a), MEOA (b) and di-epoxide linoleic acid (c).

linoleic acid Fig. 11b. The distinguishable groups are the protons of the terminal methyl of the fatty acid chain. The signals at 0.88–0.86 ppm referred to the methylene group (–C*H*$_3$) of linoleic acid Fig. 11a which also appear in MEOA 0.86–0.88 ppm and di-epoxide linoleic acid 0.88–0.92 ppm Fig. 10b and c next to the terminal methyl (–C*H*$_2$) at 1.30–2.77 ppm of linoleic acid, 1.29–2.33 of MEOA and 1.34–2.36 ppm of di-epoxide linoleic acid.

However, the methane proton signals (–C*H*═C*H*–) were shifted upfield at about 5.35–5.36 ppm of linoleic acid and 5.38–5.49 ppm of MEOA (Hwang and Erhan, 2006) while disappeared in di-epoxide linoleic acid. Another distinctive feature is the hydrolxyl proton (–COO*H*) of the carboxylic acid at about 7.27 ppm.

4. Conclusion

From the present study it is evident that hydrogen peroxide is the most critical parameter influencing the chemo-enzymatic mono-epoxidation reaction. An increase in the hydrogen peroxide amount has a strong effect on the reaction kinetics; however, a large excess of hydrogen peroxide results in the accumulation of peracid in the final product.

Acknowledgment

We would like to thank UKM and the Ministry of Science and Technology for research grants UKM-GUP-NBT-08-27-113 and UKM-ST-06-FRGS0113-2009.

References

Abdullah, B.M., Salimon, J., 2009. Physicochemical characteristics of Malaysian rubber (Hevea Brasiliensis) seed oil. European Journal of Scientific Research 31, 437–445.

Adhvaryu, A., Erhan, S.Z., 2002. Epoxidized soybean oil as a potential source of high-temperature lubricants. Industrial Crops and Products 15, 247–254.

Ahmad, S., Ashraf, S.M., Hasnat, A., 2002. Studies on corrosion protective epoxidized oil modified DGEBA epoxy paint. Paintindia 52, 50–52.

Benaniba, M.T., Belhaneche-Bensemra, N., Gelbard, G., 2003. Stabilization of PVC by Epoxidized Sunflower oil in the presence of Zinc and Calcium Stearates. *Polymer Degradation and Stability* 82, 245–249.

Doll, K.M., Sharma, B.K., Erhan, S.Z., 2007. Synthesis of branched methyl hydroxy stearates including an ester from bio-based levulinic acid. Industrial and Engineering Chemistry Research 46, 3513–3519.

Du, G., Tekin, A., Hammond, E.G., Woo, L.K., 2004. Catalytic epoxidation of methyl linoleate. Journal of American Oil Chemical Society 81, 477–480.

Hwang, H-S., Erhan, S.Z., 2006. Synthetic lubricant basestocks from epoxidezed soybean oil and Guerbet alcohols. Industrial Crops and Products 23, 311–317.

John, J., Bhattacharya, M., Turner, R.B., 2002. Characterization of polyurethane foams from soybean oil. Journal of Applied Polymer Science 86, 3097–3107.

Joseph, R., Madhusoodhanan, Alex, R., Varghese, S., George, K.E., Kuriakose, B., 2004. Studies on epoxidised rubber seed oil as secondary plasticiser/stabiliser for polyvinyl chloride. Plastics Rubber and Composites 33, 217–222.

Klaas, R., Warwel, S., 1997. Lipase-catalyzed preparation of peroxy acids and their use for epoxidation. Journal of Molecular Catalysis A: Chemical 117, 311–319.

Mason, R.L., Gunst, R.F., Hess, J.L., 1989. Statistical Design and Analysis of Experiments with Applications to Engineering and Science. Wiley, New York.

Meyer, P-P., Techaphattana, N., Manundawee, S., Sangkeaw, S., Junlakan, W., Tongurai, C., 2008. Epoxidation of soybean oil and *Jatropha* oil. Thammasat International Journal of Science Technology 13, 1–5.

Orellana-Coca, C., Camocho, S., Adlercreutz, D., Mattiasson, B., Hatti-Kaul, R., 2005. Chemo-Enzymatic epoxidation of Linoleic Acid: Parameters influencing the reaction. European Journal of Lipid Science Technology 107, 864–870.

Ruesch, M., Warwel, S., 1999. Complete and Partial Epoxidation of Plant Oils by Lipase-Catalyzed Perhydrolysis. Industrial Crops and Products 9, 125–132.

Socrates, G., 2001. Infrared and Raman characteristic group frequencies: Tables and charts. John Wily & Sons Ltd., Chichester, England, 3rd ed..

Wanasundara, N.U., Shahidi, F., 1999. Concentration of omega 3-polyunsaturated fatty acids of seal blubber oil by urea complexation: optimization of reaction conditions. Food Chemistry 65, 41–49.

Warwel, S., Bruese, F., 2004. Glucamine-based gemini surfactants II: gemini surfacntants from long-chain N-alkyl glucamines and epoxy resins. Journal of Surfactants Detergents 7, 187–193.

Warwel, S., Klaas, M.R.G., 1995. Chemo-enzymatic epoxidation of unsaturated carboxylic acids. Journal of Molecular Catalysis B: Enzymatic 1, 29–35.